Journal of Alloys and Compounds 703 (2017) 210–215

Contents lists available at ScienceDirect

Journal of Alloys and Compounds

journal homepage: http://www.elsevier.com/locate/jalcom

Critical behavior study of the spin ordering transition in RVO_3 (R = Ce, Pr, Nd, Sm, Gd, Er) by means of *ac* photopyroelectric calorimetry

A. Oleaga [a, *], V. Shvalya [a, b], V. Liubachko [a, b], G. Balakrishnan [c], L.D. Tung [c, 1], A. Salazar [a]

[a] Departamento de Física Aplicada I, Escuela Técnica Superior de Ingeniería, Universidad del País Vasco UPV/EHU, Alameda Urquijo s/n, 48013, Bilbao, Spain
[b] Institute for Solid State Physics and Chemistry, Uzhgorod University, 88000, Uzhgorod, Ukraine
[c] Department of Physics, University of Warwick, Coventry, CV4 7AL, UK

ARTICLE INFO

Article history:
Received 3 January 2017
Accepted 31 January 2017
Available online 2 February 2017

Keywords:
Orthovanadates
Spin-ordering
Phase transitions
Critical behavior
Universality class

ABSTRACT

The thermal diffusivity of RVO_3 single crystals (R = Ce, Pr, Nd, Sm, Gd, and Er) has been measured with an *ac* photopyroelectric calorimetry in the region in which the G-type orbital ordering and C-type spin ordering take place. Detailed measurements in the close neighbourhood of the spin ordering temperature have allowed to extract the critical parameter α and the critical ratio A^+/A^- for this transition. While the samples containing Ce, Nd, Sm and Er belong to the 3D-XY universality class (showing that the spins have an easy plane anisotropy), the sample with Gd, which is known to present a clear easy axis, belongs to the 3D-Ising class. Finally, $PrVO_3$ shows an effective isotropic behavior, as the critical parameters found agree with the 3D-Heisenberg class.

1. Introduction

RVO_3 family of vanadium oxides (R being a rare earth ion from La to Lu and Y) has been extensively studied along the last twenty years because of the very interesting magnetic and electronic properties they present due to spin-charge-orbital coupling. Everything started with the study of anomalous diamagnetism in $LaVO_3$ [1] followed by the discovery of a magnetization reversal phenomena in several compounds of the family [2–4] and the more recent finding of multiferroic properties [5]. A wide variety of studies on the crystallographic and magnetic properties have been developed for samples with different rare earth ions showing the similarities and, specially, the variety of the interactions and their couplings depending on the particular ion.

These orthovanadates have in common with manganites that they are both correlated electron systems, experiencing a Jahn-Teller interaction which is weaker in the first group (the orbital-active electrons belong to the t_{2g} orbital in this case while in manganites it is e_g). The relationship among spin, orbital and lattice degrees of freedom is more subtle and complex in the vanadates [6,7]. All members of the series RVO_3 crystallize in the *Pbnm* space group at room temperature and experience, on lowering the temperature, first an orbital ordering transition together with a lattice distorsion induced by the collective Jahn-Teller coupling (which leads to a monoclinic phase) and, below, a spin-ordering one, both of them continuous, with the exception of $LaVO_3$ where the spin ordering precedes the orbital ordering and for which the latter has a first order character [4,8,9]. A particular case is $CeVO_3$, where, depending on the particular crystal used for the study, both situations can appear [8–11]. Different studies have made it clear that the orbital ordering is of the G-type while the spin ordering is of the C-type, which means that the V^{3+} spins are antiferromagnetically ordered in the *ab* plane while ferromagnetically aligned along the *c* axis. From $DyVO_3$ to $LuVO_3$ there is still another transition at a much lower temperature which is a concomitant orbital and spin ordering transition, with a first order character. The new spin ordering is now G-type with an antiferromagnetic coupling between the V^{3+} spins in all directions while the new orbital ordering is C-type [9,12,13].

Besides the general picture presented above for all RVO_3, more detailed studies have been undertaken for particular members of the family, showing that there are important differences in the details among them, starting with the position of the different transitions, which is clearly shown in Fig. 1 from Ref. [9]. In particular, the temperature of the first spin ordering transition is reduced as the atomic radius of the rare earth ion is decreased, possibly due to the increase of the exchange interaction, while the

* Corresponding author.
E-mail address: alberto.oleaga@ehu.es (A. Oleaga).
[1] Present address: Department of Physics and Astronomy, University College London, Gower Street, London, WC1E 6BT, UK.

http://dx.doi.org/10.1016/j.jallcom.2017.01.361
0925-8388/

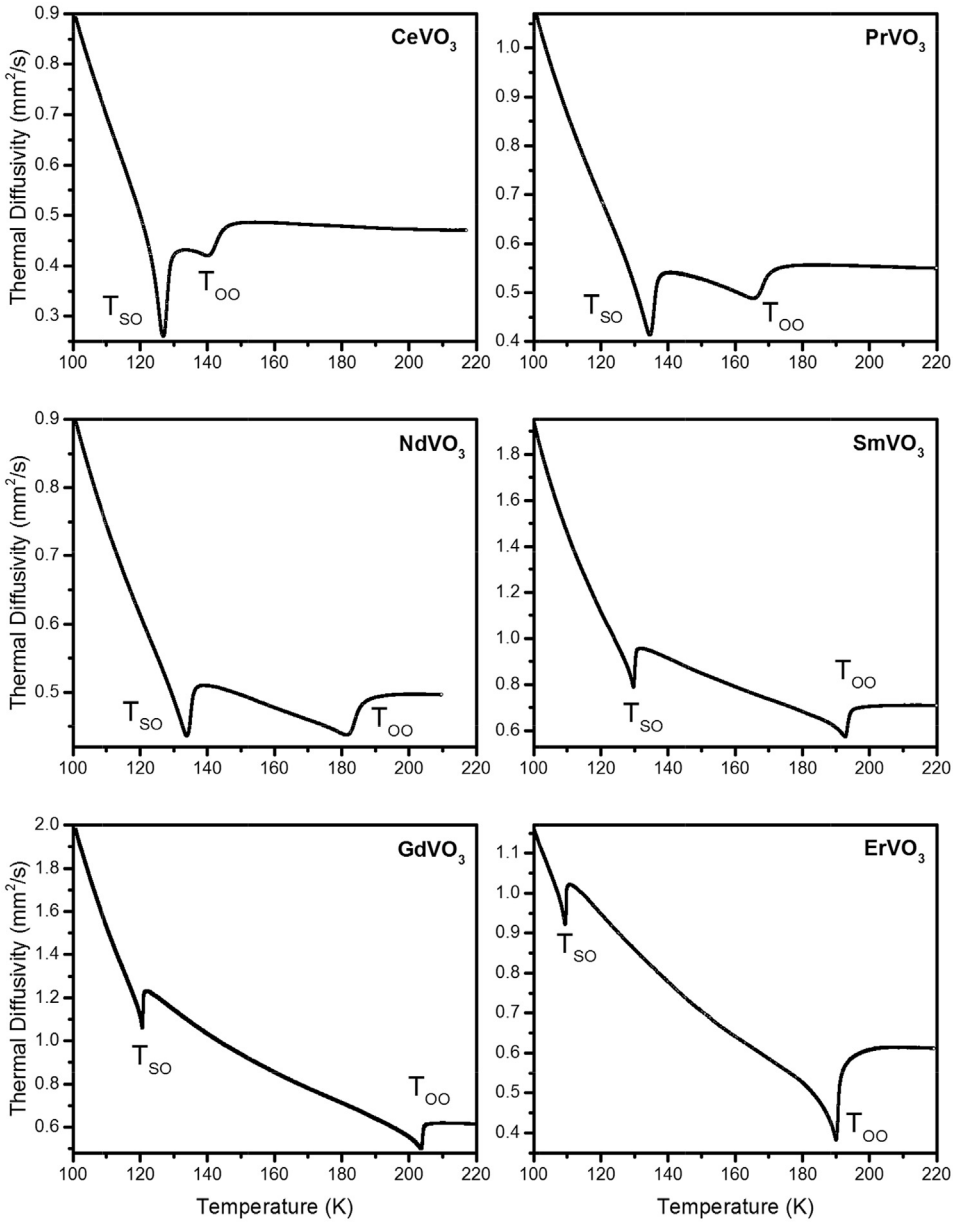

Fig. 1. Thermal diffusivity as a function of temperature for RVO_3 (R = Ce, Pr, Nd, Sm, Gd, and Er) showing the orbital ordering transition at T_{OO} and the spin ordering one at T_{SO}.

higher orbital ordering transition temperature reaches a maximum for an intermediate value of that radius, which has been suggested to be due to the competition between the increase of the orbital exchange interaction and the suppression of the Jahn-Teller instability [15]. Other differences arise in the particular direction in which the V^{3+} spins are placed within the C-type spin ordered phase, which has not been studied for all ions yet. Literature results point to differences between the two big groups (La to Tb, Dy to Lu) [16], some cantings have been proposed [12,17–19] and in some cases particular easy axes have been found for $SmVO_3$ [20] or $GdVO_3$ [21], while PrVO3 has been found to behave as a disordered antiferromagnet with random fields [22].

The aim of this work is to shed some light on this last issue: how spins are displayed in the C-type spin ordered state of RVO_3 (R = Ce, Pr, Nd, Sm, Gd, Er). An interesting support can be brought from the critical behavior theory and the universality classes theorized within the framework of renormalization group theory. In the critical region around a second order magnetic transition, several physical magnitudes behave critically after the following equations, where t is a reduced temperature $t = (T\text{-}T_C)/T_C$ and T_C the temperature of the transition [23]:

-specific heat $c_p(T) \sim A^{\pm} |t|^{-\alpha}$ (A^- for $T < T_C$, A^+ for $T > T_C$), (1)

-spontaneous magnetization $M_S(T) \sim |t|^{\beta}$ ($T < T_C$), (2)

-inverse of initial susceptibility $\chi_0^{-1}(T) \sim |t|^{\gamma}$ ($T > T_C$), (3)

just to cite some of them. Different sets of values of the exponents (α, β, γ) correspond to different models (universality classes) which have been theoretically developed after a certain expression of the Hamiltonian describing the physical system. Table 1 contains the most relevant universality classes for magnetic systems, for which the values of the exponents have been found by different methods

Table 1
Main universality classes for magnetic systems [24–27].

Universality class	α	β	γ	A^+/A^-
Mean-field Model	0	0.5	1.0	–
3D-Ising	0.11	0.3265	1.237	0.53
3D-XY	−0.014	0.34	1.30	1.06
3D-Heisenberg	−0.115	0.365	1.386	1.52

[24–27]. The mean field model is equivalent to the classical Landau model and is based on long-range interactions. The other three models describe the (anti)ferromagnetic phenomena on the basis of short range interactions among the spins: the Heisenberg model corresponds to an isotropic (anti)ferromagnetic material, XY model is of application when there is an easy plane for the magnetization and the Ising model is applicable when there is a uniaxial anisotropy. As can be seen from Table 1, in the case of the short range models, the specific heat is the physical magnitude with which the discrimination among models is more precise as the values of β and γ (extracted from magnetic measurements) are too similar for the different classes. Thus, the purpose of this work is to study the thermal properties of RVO_3 in the vicinity of the C-type spin ordering transition, extract the critical parameters α and A^+/A^-, identify the universality class to which they belong and discuss the corresponding physical interpretation about the orientation of the spins.

2. Samples and experimental techniques

Single crystals of RVO_3 (R = Ce, Pr, Nd, Sm, Gd, and Er) were prepared and checked following the procedure that is thoroughly explained in Ref. [4]. Slabs of plane parallel faces were then prepared with thicknesses ranging between 500 and 535 μm for our measurements. The critical parameters related to specific heat can also be found from some other magnitudes which have the same critical behavior in the vicinity of the critical temperature. One of them is the inverse of thermal diffusivity D, related to specific heat by

$$c_p = \frac{K}{\rho D} \tag{4}$$

(K stands for thermal conductivity and ρ for density) provided that thermal conductivity does not present any singularity at the transition, which is the case, as will be justified later. What will be measured, then, is the through-thickness thermal diffusivity in all samples for this study.

In order to perform a high resolution temperature sweep of thermal diffusivity in the region of interest for each RVO_3, a combination of an *ac* photopyroelectric technique in the back-detection configuration with $LiTaO_3$ as a sensor and a closed cycle He cryostat has been employed. The detailed methodology of the measurements performed can be found in Ref. [28] and references therein. The temperature rates used for the measurements have been chosen between the extreme ranges of 80 and 10 mK/min depending on the absence or presence of a phase transition and the need to check its first or second order character. Low rates have been needed to ensure there was no hysteresis in particular phase transitions. The experimental curves shown in all graphs are the ones obtained experimentally, without any fitting or treatment. In the continuous runs, the relative resolution of the points is ±0.0001 mm^2/s in D and ±0.001 K in T, retrieving the precise shape of the thermal diffusivity as a function of temperature, especially around the phase transition point.

In the particular case of $CeVO_3$, magnetization measurements have been carried out in a MPMS3 VSM-SQUID by Quantum Design in order to elucidate which of the two transitions found is the magnetic one, as there is some controversy in literature and it might depend on the particular stoichiometry of the sample or valence state of the Ce ions [7,11].

3. Experimental results

Fig. 1 shows the thermal diffusivity of the six samples studied in the temperature region of interest (100–230K) where the two transitions for each sample are present as dips superimposed on the monotonous evolution of thermal diffusivity with temperature. It is perfectly settled in literature [9] that for R = Pr, Nd, Sm, Gd and Er the highest temperature transition belongs to the orbital order type while the lowest one corresponds to the ordering of the spins of the V^{3+} ions. As pointed out in the introduction, in the case of Ce some authors have attributed the same type of transitions, some others the opposite one. The relative position of our critical temperatures resembles very much those of [11], where the authors showed that the lowest one is a spin-ordering transition while the higher one is not. In order to be sure about it we have performed magnetization measurements (see Fig. 2) where it is clear that the spin ordering takes place only at the lowest transition.

Concerning the general shape of the curves shown in Fig. 1, they present a typical behavior of thermally insulating materials, where phonons are mainly responsible for heat conduction and the phonon mean free path is small at high temperatures. As the temperature is lowered from room temperature, there is a monotonous and very slow increase in thermal diffusivity, which is nearly constant till the orbital ordering takes place, which is manifested as a dip at the transition (as it happens for instance in manganites [29]). Concerning the character of these transitions, we have checked that in all six cases they are second order as no hysteresis is found when using low temperature rates, the curves perfectly superimpose on heating and cooling cycles. Going to lower temperatures, in all cases there is a quicker increase in the thermal diffusivity curve, due to the fact that the phonon mean free path starts to increase but the presence of the spin ordering transition interrupts this increase. The magnetic transition is signaled as a strong dip, whose sharpness depends on the presence of one or other rare earth ion. This kind of dips is customarily found in magnetic transitions [30–33]. Again, we have carefully checked the character of the transitions using low temperature rates, finding a complete superposition of the curves in heating and cooling runs, confirming that they are all continuous. From then on, thermal

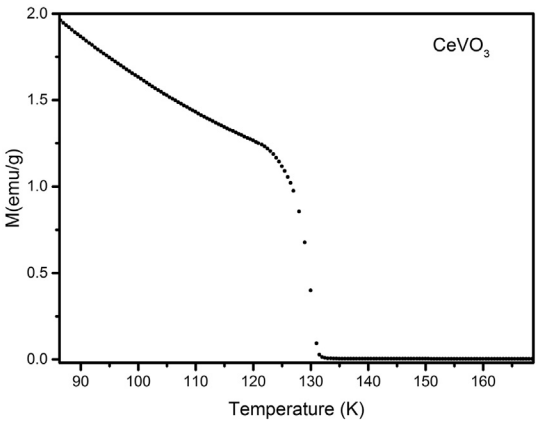

Fig. 2. Magnetization as a function of temperature for $CeVO_3$ measured in a field-cooled state using a magnetic field of 100 Oe.

diffusivity quickly increases as temperature keeps on being lowered due to the fast increase in phonon mean free paths.

One small additional comment about the character of the spin ordering transition in $CeVO_3$. In literature, it is said to be first order [8,9] but this is in the cases in which the orbital ordering transition appears below the spin ordering, as it happens with $LaVO_3$ [9]. Goodenough et al. [12] have argued why when the orbital ordering transition is above the spin ordering, both transitions are second order. They affirm that a first-order transition at the Néel temperature T_N is usually found where the spin order is coupled to a cooperative orbital ordering at T_{OO}, for which T_N must be very close to T_{OO}. In our case, the separation seems to be enough to behave as the rest of the RVO_3 samples.

4. Critical behavior: fittings and discussion

As explained in the introduction, the critical behavior theory assess that, at a second order phase transition, specific heat fulfills Eq. (1). From Eq. (4) it follows that the specific heat and the inverse of thermal diffusivity will have the same critical behavior provided that the thermal conductivity does not present any singularity at the phase transition, which is the case in this family, as shown in Ref. [7]. This implies that we can use the curves shown in Fig. 1 to extract information about the universality class to which the spin ordering transitions might belong and thus obtain more information about the ordering of those spins.

In particular, the equation that we are going to use to fit the inverse of the thermal diffusivity data presented in Fig. 1 will be the well known [32,34,35].

$$\frac{1}{D} = B + Ct + A^{\pm}|t|^{-\alpha}\left(1 + E^{\pm}|t|^{0.5}\right) \tag{5}$$

where t is the reduced temperature, superscripts $+$ and $-$ stand for $T > T_C$ and $T < T_C$ respectively. The linear term represents the regular contribution to the inverse of the thermal diffusivity, while the last term represents the anomalous contribution at the second order phase transition; the term in parenthesis is a small correction term introduced based on experiments and theory [36,37] but which is not always necessary. Scaling laws require that there is a unique critical exponent α for both branches and rigorous application states that constant B needs also be the same. The experimental data were simultaneously fitted for $T > T_C$ and $T < T_C$ with a non-linear least square routine using a Levenberg-Marquardt method. The details of the fitting procedure can be found in Refs. [34,35].

Figs. 3 and 4 show the experimental curves, the fitted curves to Eq. (5), as well as the deviation curves, which show the difference between the experimental points and the fitted curves, in percentage. Table 2 contains the critical parameters obtained from the fittings for the six samples, together with the fitted range and the root mean square value. Comparing the critical parameters obtained from this analysis, four of the samples belong to the 3D-XY universality class (those with Ce, Nd, Sm and Er) while the one with Pr belongs to the Heisenberg class and with Gd is very close to the Ising class, revealing the different magnetic properties of RVO_3 containing a different rare earth ion.

If we simply take into account the C-type magnetic ordering which, as a rule, is assumed for the spin ordering transition above 100K in *R*VO3, the spins are antiferromagnetically aligned on the *ab* plane while these planes are ferromagnetically aligned along the *c*-axis. Hence, the only possible universality classes would be 3D-XY (easy plane magnetization) or 3D-Ising (if there were an easy axis on the *ab* plane). Any significant canting or the presence of coupling effects would deviate the critical parameters from the theoretical values as manifested in other magnetic transitions [33,35]. Four of the samples (R = Ce, Nd, Sm and Er) agree with the easy plane description, giving critical exponents very close to the theoretical ones for the 3D-XY plane ($\alpha_{theor} = -0.014$, $A^+/A^-_{theor} = 1.06$), within a range -0.014 to -0.018, 1.02 to 1.08 (see Table 2). In all cases these were the best fittings and the possibility of finding better fittings for other models (such as 3D-Heisenberg, 3D-Ising or Mean Field universality classes) was checked and discarded. These results in $CeVO_3$ are in agreement with the magnetic structure study developed by Reehuis et al. [11]. On the other hand, Nguyen et al. [38] suggested for this material a spin-canted ferromagnetic component superimposed to the antiferromagnetic ordering, which is not revealed in our study. But then, that sample was a polycrystal where the orbital ordering transition was below the spin ordering transition, so the comparisons are not direct.

Turning our attention to $NdVO_3$, a neutron diffraction performed

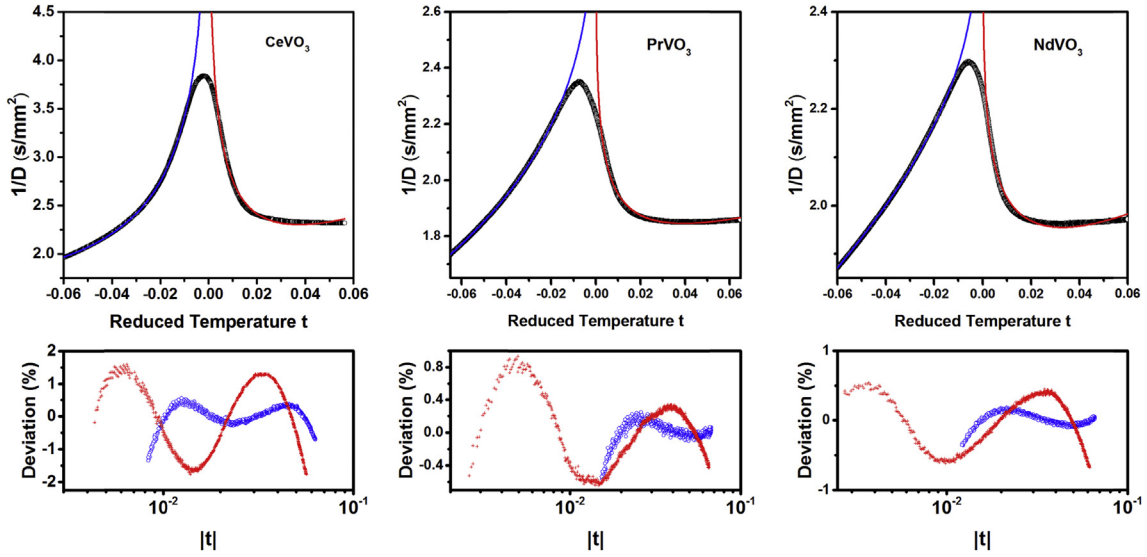

Fig. 3. Above: Inverse of thermal diffusivity as a function of the reduced temperature in the near vicinity of the critical temperature for $CeVO_3$, $PrVO_3$, and $NdVO_3$. The points correspond to the experimental values while the continuous lines are the fit to Eq. (5). Below: Deviation curves (difference between the experimental and the fitted valued, in percentage). Crosses are for data above T_N, dots for data below T_N.

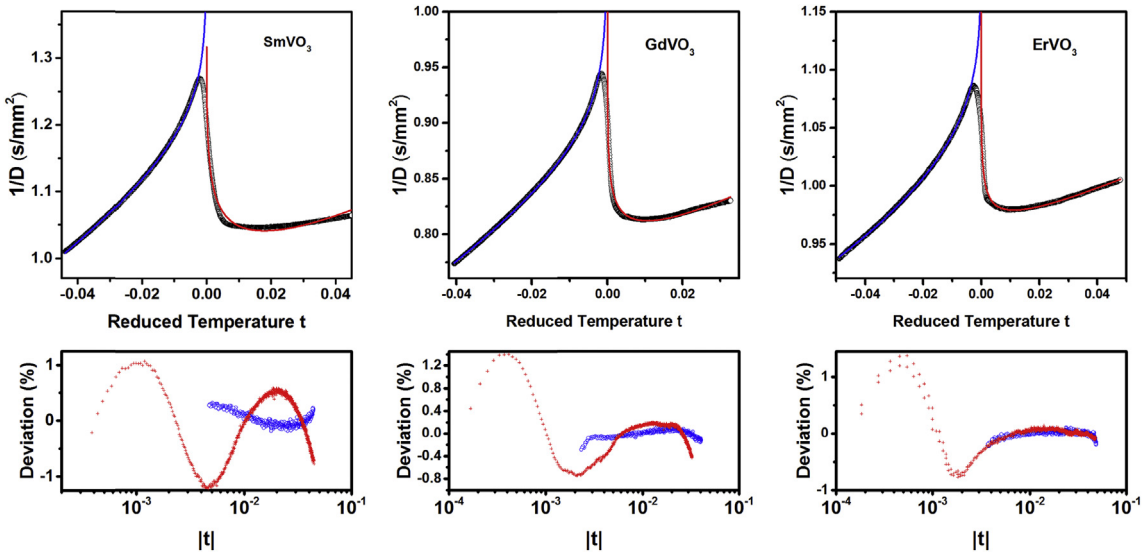

Fig. 4. Above: Inverse of thermal diffusivity as a function of the reduced temperature in the near vicinity of the critical temperature for $SmVO_3$, $GdVO_3$, and $ErVO_3$. The points correspond to the experimental values while the continuous lines are the fit to Eq. (5). Below: Deviation curves (difference between the experimental and the fitted valued, in percentage). Crosses are for data above T_N, dots for data below T_N.

Table 2
Critical parameters, fitting ranges, quality of the fittings (given by the root mean square value) and universality class to which the samples are attributed.

R ion	α	A^+/A^-	t_{min}-t_{max} $T < T_N$	t_{min}-t_{max} $T > T_N$	R^2	Universality Class
Ce	-0.018 ± 0.011	1.02	6.3×10^{-2}-8.3×10^{-3}	4.3×10^{-3}-5.6×10^{-2}	0.99734	3D-XY
Pr	-0.11 ± 0.01	1.48	6.7×10^{-2}-1.4×10^{-2}	2.0×10^{-3}-6.6×10^{-2}	0.99811	3D-Heisenberg
Nd	-0.017 ± 0.002	1.05	6.4×10^{-2}-1.2×10^{-2}	2.8×10^{-3}-6.2×10^{-2}	0.99670	3D-XY
Sm	-0.016 ± 0.002	1.06	4.4×10^{-2}-4.7×10^{-3}	3.5×10^{-4}-4.4×10^{-2}	0.99370	3D-XY
Gd	0.07 ± 0.01	0.70	4.1×10^{-2}-2.3×10^{-3}	1.6×10^{-4}-3.3×10^{-2}	0.99753	Close to 3D-Ising
Er	-0.014 ± 0.006	1.08	4.9×10^{-2}-3.6×10^{-3}	9×10^{-5}-4.8×10^{-2}	0.99761	3D-XY

in Ref. [14] showed that the magnetic moments order on the *ab* plane without any canting, which is compatible with the 3D-XY result obtained here. In the case of $SmVO_3$, there is a very interesting work where the magnetic susceptibility along the different axis has been measured [20] with the result that the *a*-axis is an easy axis, while for *b* the susceptibility is intermediate and *c* is the hard axis. We have specially checked the pertinence of an Ising-model in the fitting of our experimental curve but no fitting could be found for that universality class, the 3D-XY was the only one found. This would mean that the difference in magnetization along *a* and *b* axis is not too strong. Lastly, in the case of $ErVO_3$, in the work performed on its magnetic structure by Reehuis et al. [39], they found that in the C-type magnetic structure, the spins were indeed on the *ab* plane, in agreement with our results.

But there are other two samples where the fitted results do not agree with the 3D-XY universality class. In the case of $PrVO_3$ they unambiguously correspond to the 3D-Heisenberg model (the obtained parameters are the theoretical ones with very small errors and very good deviation curves), which is incompatible with the assumed common spin ordering in RVO_3. But the magnetic properties of this particular member of the family have already been found to be very special when single crystals (as is our case) and not polycrystalline samples are studied [22]. The author in that work proposes that $PrVO_3$ should be considered a disorder antiferromagnet with an effective random field, whose origin might be an orbital quantum fluctuation. There is no theorized universality class for magnetic transitions with these effects so we have not been able to check other models than the common ones. Our conclusion is that the Heisenberg model is an "effective" universality class, which means that the magnetic properties might be somewhat equivalent to an isotropic antiferromagnet.

In the last case, $GdVO_3$, the critical parameters obtained point to the 3D-Ising model ($\alpha_{theor} = +0.11$, $\alpha_{fitted} = +0.07$, $A^+/A^-_{theor} = 0.53$, $A^+/A^-_{fitted} = 0.70$), which would indicate the presence of an easy axis. A complete work on the magnetic properties of this material [21] has showed that it presents magnetic properties which make it quite different from the rest of the series and that, in particular, the *a* axis is indeed an easy axis, in agreement with our results.

5. Conclusions

The critical behavior of the spin ordering transition for RVO_3 (R = Ce, Pr, Nd, Sm, Gd, and Er) has been studied by means of *ac* photopyroelectric calorimetry, measuring with detail the thermal diffusivity in the close neighbourhood of the critical temperature and extracting the critical parameter α and the critical ratio A^+/A^-. The samples containing Ce, Nd, Sm and Er belong to the 3D-XY universality class, showing that the spins have an easy plane anisotropy. The sample with Gd belongs to the 3D-Ising class, in agreement with an easy-axis anisotropy reported in literature. Finally, the sample with Pr shows an effective isotropic behavior, as the 3D-Heisenberg class is of application, surely due to the disordered antiferromagnetic properties that it displays.

Acknowledgements

This work has been supported by UPV/EHU (UFI11/55). The work at the University of Warwick was supported by a grant from the

EPSRC, UK, EP/M028771/1. The authors thank for technical and human support provided by SGIker of UPV/EHU. V. Shvalya and V. Liubachko thank the Erasmus Mundus programme “ACTIVE” for their grants.

References

[1] N. Shirakawa, M. Ishikawa, Jpn. J. Appl. Phys. 30 (1991) L755.
[2] Y. Ren, T.T.M. Palstra, D.I. Khonskii, E. Pellegrin, A.A. Nugroho, A.A. Menovsky, G.A. Sawatzky, Nature 296 (1998) 441.
[3] J.Q. Yan, J.S. Zhou, J.B. Goodenough, Phys. Rev. 72 (2005) 094412.
[4] L.D. Tung, M.R. lees, G. Balakrishnan, D. McK Paul, Phys. Rev. B 75 (2007) 104404.
[5] Q. Zhang, K. Singh, C. Simon, L.D. Tung, G. Balakrishnan, V. Hardy, Phys. Rev. B 90 (2014) 024418.
[6] J. Fujioka, T. Yasue, S. Miyasaka, Y. Yamasaki, T. Arima, H. Sagayama, T. Inami, K. Ishii, Y. Tokura, Phys. Rev. B 82 (2010) 144425.
[7] J.Q. Yan, J.S. Zhou, J.B. Goodenough, Phys. Rev. Lett. 93 (2004) 235901.
[8] Y. Ren, A.A. Nugroho, A.A. Menovsky, J. Strempfer, U. Rütt, F. Iga, T. Takabatake, C.W. Kimball, Phys. Rev. B 67 (2003) 011407.
[9] S. Miyasaka, Y. Okimoto, M. Iwama, Y. Tokura, Phys. Rev. B 68 (2003), 100406(R).
[10] A. Muñoz, J.A. Alonso, M.T. Casais, M.J. Martinez-Lope, J.L. Martinez, M.T. Fernandez-Diaz, Phys. Rev. B 68 (2003) 144429.
[11] M. Reehuis, C. Ulrich, P. Pattison, M. Miyasaka, Y. Tokura, B. Keimer, Eur. Phys. J. B 64 (2008) 27.
[12] J.B. Goodenough, J.S. Zhou, J. Mater. Chem. 17 (2007) 2394.
[13] M.H. Sage, G.R. Blake, C. Marquina, T.T.M. Palstra, Phys. Rev. B 76 (2007) 195102.
[14] M. Reehuis, C. Ulrich, P. Pattison, B. Ouladdiaf, M.C. Rheinstädter, M. Ohl, L.P. Regnault, M. Miyasaka, Y. Tokura, B. Keimer, Phys. Rev. B 73 (2006) 094440.
[15] S. Miyasaka, J. Fujioka, M. Iwama, Y. Okimoto, Y. Tokura, Phys. Rev. B 73 (2006) 224436.
[16] R.V. Yusupov, D. Mihailovic, C.V. Colin, G.R. Blake, T.T.M. Plastra, Phys. Rev. B 81 (2010) 075103.
[17] H.C. Nguyen, J.B. Goodenough, Phys. Rev. B 52 (1995) 324.
[18] Y. Ren, T.T.M. Palstra, D.I. Khonskii, A.A. Nugroho, A.A. Menovsky, G.A. Sawatzky, Phys. Rev. B 62 (2000) 6577.
[19] G. Ulrich, G. Khaliullin, J. Sirker, M. Reehuis, M. Ohl, M. Miyasaka, Y. Tokura, B. Keimer, Phys. Rew. Lett. 91 (2003) 257202.
[20] R.D. Jonhson, C.C. Tang, I.R. Evans, S.R. Bland, D.G. Free, T.A.W. Beale, P.D. Hatton, L. Bouchenoire, D. Prabhakaran, A.T. Boothroyd, Phys. Rev. B 85 (2012) 224102.
[21] L.D. Tung, Phys. Rev. B 73 (2006) 024428.
[22] L.D. Tung, Phys. Rev. B 72 (2005) 054414.
[23] H.E. Stanley, Introduction to Phase Transitions and Critical Phenomena, Oxford University Press, 1971.
[24] R. Guida, J. Zinn-Justin, J. Phys. A Math. Gen. 31 (1998) 8103.
[25] M. Campostrini, M. Hasenbusch, A. Pelisseto, P. Rossi, E. Vicari, Phys. Rev. B 63 (2001) 214503.
[26] M. Campostrini, M. Hasenbusch, A. Pelisseto, P. Rossi, E. Vicari, Phys. Rev. B 65 (2002) 144520.
[27] M. Hasenbusch, Phys. Rev. B 82 (2010) 174434.
[28] A. Oleaga, A. Salazar, A. Kohutych, Yu. Vysochanskii, J. Phys. Condens. Matter 23 (2011) 025902.
[29] A. Salazar, A. Oleaga, D. Prabhakaran, Int. J. Thermophys. 25 (2004) 1269.
[30] M. Marinelli, F. Mercuri, D.P. Belanger, Phys. Rev. B 51 (1995) 8897.
[31] M. Massot, A. Oleaga, A. Salazar, D. Prabhakaran, M. Martin, P. Berthet, G. Dhalenne, Phys. Rev. B 77 (2008) 134438.
[32] A. Oleaga, A. Salazar, Yu. Bunkov, J. Phys. Condens. Matter 26 (2014) 096001.
[33] A. Oleaga, A. Salazar, D. Skrzypek, J. Alloys Compd. 629 (2015) 178.
[34] A. Oleaga, V. Shvalya, A. Salazar, I. Stoika, Yu. M. Vysochanskii, J. Alloys Compd. 694 (2017) 808–814.
[35] A. Oleaga, A. Salazar, D. Prabhakaran, J.G. Cheng, J.S. Zhou, Phys. Rev. B 85 (2012) 184425.
[36] M. Marinelli, F. Mercuri, U. Zammit, R. Pizzoferrato, F. Scudieri, D. Dadarlat Phys. Rev. B 49 (1994) 9523.
[37] A. Kornblit, G. Ahlers, Phys. Rev. B 11 (1975) 2678.
[38] H.C. Nguyen, J.B. Goodenough, J. Solid State Chem. 119 (1999) 24.
[39] M. Reehuis, C. Ulrich, K. prokes, S. Mat'as, J. Fujioka, S. miyasaka, Y. Tokura, B. Keimer, Phys. Rev. B 83 (2011) 064404.